Electronic Supplementary Material (ESI) for Physical Chemistry Chemical Physics.

Molecular Insights into the Enhanced Rate of CO_2 Absorption to Produce Bicarbonate in Aqueous 2-amino-2-methyl-1-propanol

(Supporting Information)

Haley M. Stowe [a] *and Gyeong S. Hwang*[a,b,*]

[a]Materials Science and Engineering Program and [b]McKetta Department of Chemical Engineering, University of Texas at Austin, Austin, Texas 78712, USA.

*Author to whom correspondence should be addressed: Tel: 1-512-471-4847, Fax: 1-512-471-7060, E-mail: gshwang@che.utexas.edu

Free Energy Calculations Using Metadynamics

To calculate the free energy barriers for the bicarbonate formation reactions in Section 2.1 and proton abstraction reactions in Section 2.3, we used metadynamics via the PLUMED plugin[1] from Car-Parrinello molecular dynamics simulations within the CPMD code[2]. In metadynamics, a bias potential, which is a function of collective variables that describe the progression of the reaction, is added to the free energy to prevent the system from sampling previous configurations. These potential hills are then summed to construct the free energy surface with respect to the chosen collective variables. Here, we used hills of width 0.4 a.u. and height of 1 kcal/mol, which were deposited every 200 timesteps (where each timestep was 0.17 fs) over a trajectory of 54 ps; a trajectory of 27 ps was used for the $OH^- + CO_2 \rightarrow HCO_3^-$ reaction. Restraining potentials to prevent migration of OH^-, HCO_3^- and CO_2 away from the (protonated) amine are listed in Table S1; a spring constant of 0.05 a.u. was employed for each constraint.

In all three systems, there are 29 H_2O molecules per OH^- molecule. Previous works examining the solvation structure and diffusivity of OH^- in aqueous solution have found that including more than approximately 30 H_2O molecules per OH^- does not significantly affect its behavior, as it is sufficiently solvated.[3,4] However, since we also have a CO_2 molecule in the system, we performed further calculations to examine the effect of the system size on the difference in energies between the final and initial states. We performed classical MD simulations in the NVT ensemble with the fixed OH^-+CO_2 or HCO_3^- molecules (their configurations corresponding to the initial/final states obtained from the metadynamics-biased Car-Parinello MD simulations) and 29 (58) H_2O molecules in a cubic periodic box of side length 9.92 (12.28) Å. Classical MD simulations were used in order to sufficiently sample multiple hydrogen bond networks which can impact the energies calculated; the total energies were averaged over a 1.5 ns trajectory. The predicted total energy change between the initial/final states differed by less than 1 kcal mol^{-1} in the two systems.

The revPBE functional was used for the free energy barrier predictions. As previously reported, BLYP tends to predict the correct 4-fold coordination of OH^-, while PW91(revPBE) and HCTH tend to under or over predict the coordination of OH^-, thereby over and under predicting the structural diffusion, respectively.[3] Since we do not allow structural diffusion to keep the hydroxide ion relatively close to CO_2 and enhance sampling during the metadynamics-biased Car-Parrinello molecular dynamics simulations, the use of revPBE should not be a concern; note the OH^- is still fully hydrated in our initial state. Regardless, we did perform further calculations to evaluate the effect of functional on the total energy changes between the initial, transition, and final states for the $OH^- + CO_2 \rightarrow HCO_3^-$ reaction. The configurations of the initial/transition/final states are as shown in Figure S2 when structural diffusion is not allowed. As shown in Table S2, the changes in total energy are predicted to be similar. Furthermore, our interest is in comparing the free energy barriers between amine-catalyzed hydration of CO_2 in aqueous AMP and DEEA, rather than in predicting free energy barriers which can be compared to experimental values.

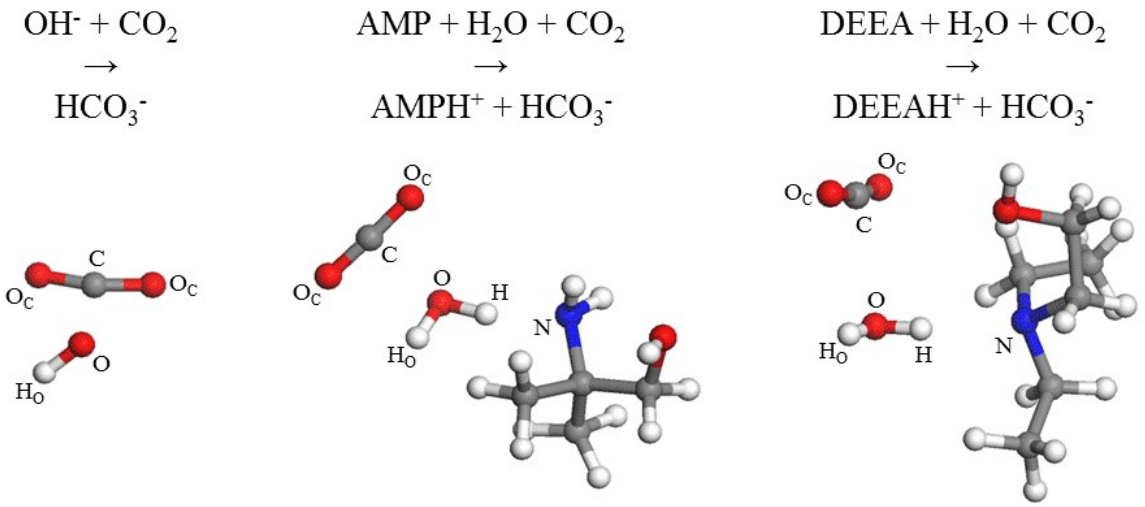

Fig S1. Structures of AMP, DEEA, H_2O/OH^-, and CO_2 with corresponding atom notation used for free energy calculations from metadynamics-biased Car-Parrinello MD simulations. Blue, red, grey and white balls represent N, O, C and H atoms, respectively.

Table S1. Restraining potentials used in free energy barrier calculations from metadynamics-biased Car-Parrinello MD simulations.

Reaction	Constraint	Lower Bound [Å]	Upper Bound [Å]
AMP(DEEA) + H_2O + CO_2 → $AMPH^+$($DEEAH^+$) + HCO_3^-	N-H distance	1.00	2.17
	O-H distance	0.90	2.86
	C-O distance	1.00	2.60
	Minimum distance between O and nearest H of surrounding H_2O	1.48	n/a
	$O\text{-}H_O$ distance	n/a	1.30
OH^- + CO_2 → HCO_3^-	C-O distance	1.00	3.50
	Distance between O and nearest H of surrounding H_2O	1.48	n/a
	$O\text{-}H_O$ distance	n/a	1.30
	Distance between O_C and nearest H of surrounding H_2O	1.48	n/a
AMP(DEEA) + H_2O → $AMPH^+$($DEEAH^+$) + OH^-	N-H distance	1.00	2.17
	O-H distance	0.90	2.17
	Distance between O and nearest H of surrounding H_2O	1.48	n/a
	$O\text{-}H_O$ distance	n/a	1.30

Table S2. Relative Total Energies (*E* in kcal mol^{-1}) for the initial (*IS*), transition (*TS*) and final (*FS*) states of the $OH^- + CO_2 \rightarrow HCO_3^-$ reaction predicted after energy optimization using PW91, HCTH, BLYP and revPBE functionals. The positions of the *IS*/*TS*/*FS* states are indicated in Figure S2. For the *TS*, the positions of the atoms in OH^- and CO_2 were constrained. Each system contains 1 OH^-, 1 CO_2 and 29 H_2O molecules in a cubic periodic box with side length 9.92 Å. Energy optimizations were performed after annealing at 313 K for approximately 5 ps, followed by quenching of the ions/electrons.

Functional	*IS*	*TS*	*FS*
PW91	0.00	0.03	-9.10
HCTH	0.00	0.05	-8.67
BLYP	0.00	0.02	-5.65
revPBE	0.00	0.04	-7.54

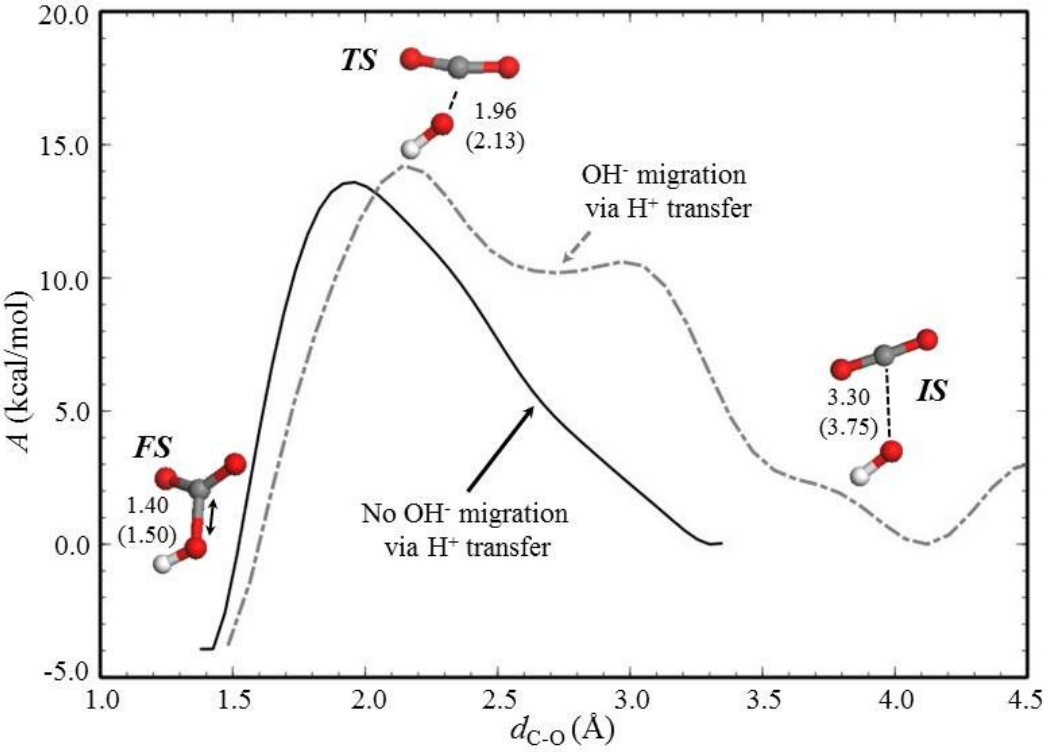

Figure S2. Free energy surface (A in kcal mol^{-1}) for the $OH^- + CO_2 \rightarrow HCO_3^-$ reaction predicted from metadynamics-biased Car-Parrinello MD simulations at 313 K. The system contains 29 H_2O, 1 OH^- and 1 CO_2 molecules in a cubic periodic box with side length 9.92 Å. The distance between C in CO_2 and O of OH^- ($d_{C\text{-}O}$) was employed as the collective variable (CV), both when OH^- diffusion via H^+ transfer is not allowed (solid black solid) and is allowed (grey dash-dotted line). Further details regarding the collective variable to allow structural diffusion of OH^- are provided in previous studies.[5] The positions of the initial (*IS*), transition (*TS*) and final (*FS*) states are also indicated, with corresponding molecular configurations both when OH^- diffusion via H^+ transfer is prevented (and allowed). The red, grey, and white balls represent O, C, and H atoms, respectively. The interatomic distances indicated are given in Å.

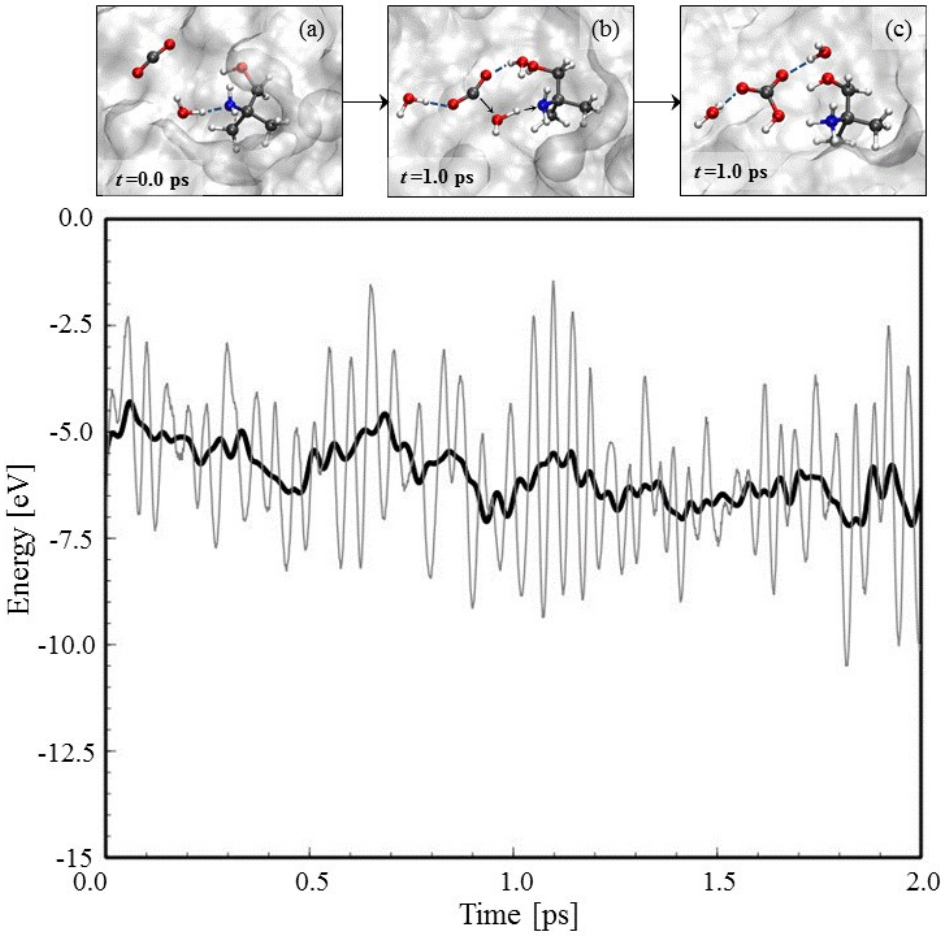

Figure S3. Variation in the total energy [eV] during the AMP + H_2O + CO_2 → $AMPH^+$ + HCO_3^- reaction from AIMD simulations at 1000 K with corresponding snapshots. The time given is in reference to when the reaction event begins; simulations were performed in the NVT ensemble for approximately 80 ps prior to the reaction event. System contains 21 H_2O, 2 AMP, and 2 CO_2 molecules in a cubic periodic box of side length 9.91 Å, corresponding to approximately 32 wt% aqueous AMP solution. Due to the small system size, 5 cases with different initial configurations were considered. Blue, red, grey and white balls represent N, O, C and H atoms, respectively. Solvent is represented by the white isosurface.

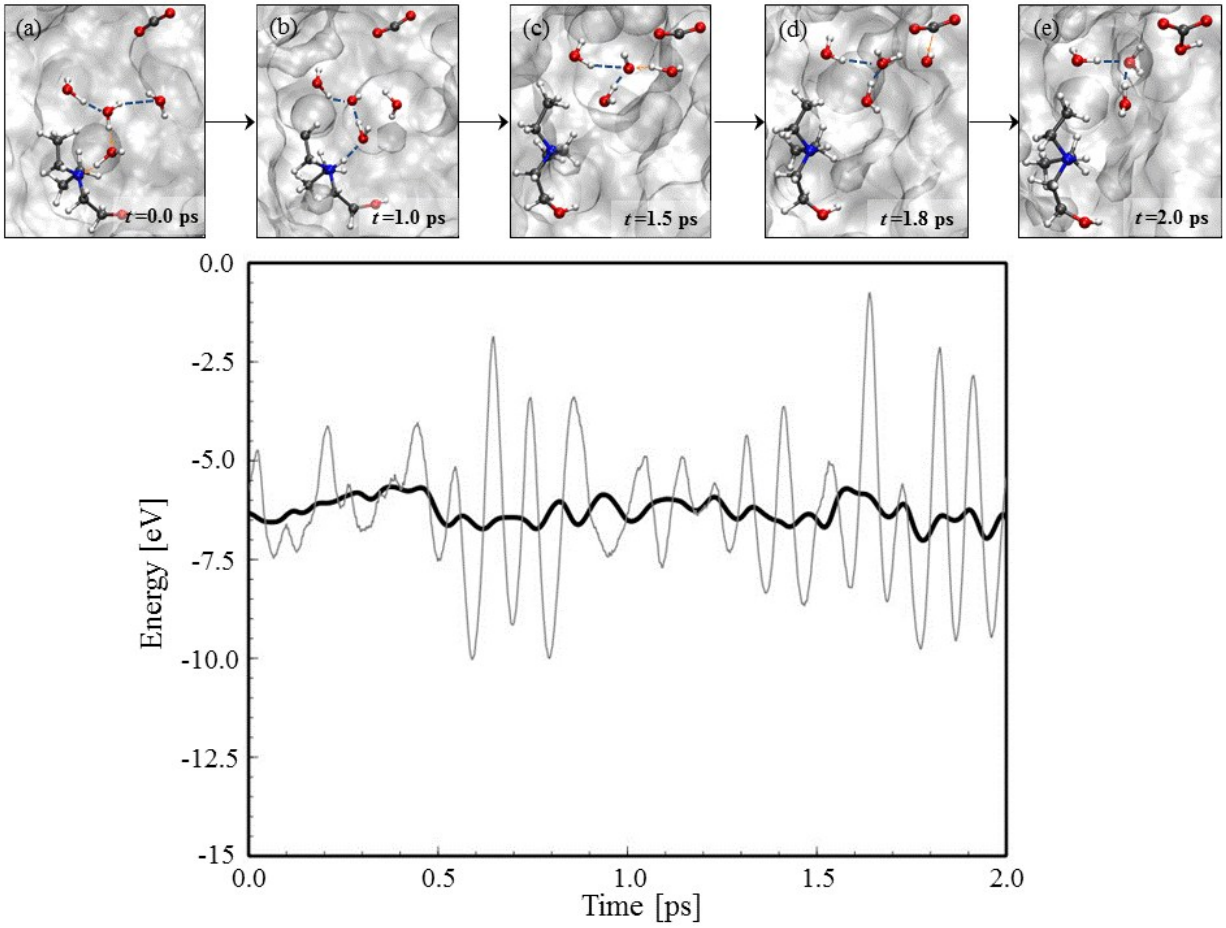

Figure S4. Variation in the total energy [eV] during the DEEA + H_2O + CO_2 → $DEEAH^+$ + HCO_3^- reaction from AIMD simulations at 1000 K with corresponding snapshots. The time given is in reference to when the reaction event begins; simulations were performed in the NVT ensemble for approximately 45 ps prior to the reaction event. System contains 20 H_2O, 2 DEEA, and 1 CO_2 molecules in a cubic periodic box of side length 10.07 Å, corresponding to approximately 38 wt% aqueous DEEA solution. Due to the small system size, 5 cases with different initial configurations were considered. Blue, red, grey and white balls represent N, O, C and H atoms, respectively. Solvent is represented by the white isosurface.

Force fields employed in this work

The total energy (E_{total}) is the sum of the bond (E_{bond}), angle (E_{angle}), torsion ($E_{torsion}$) and nonbonding energies ($E_{nonbond}$). The nonbonding energy for each pair includes Colulomb interaction and van der Waals interaction in the 12-6 Lennard-Jones form. Bond and angle energies were expressed in the harmonic form. Two different forms were used to express the torsion energies, depending on the dihedral type.

$$E_{total} = E_{bond} + E_{angle} + E_{torsion} + E_{nonbond}$$

$$E_{bond} = \sum_i k_{b,i}(r_i - r_{0,i})^2$$

$$E_{angle} = \sum_i k_{\theta,i}(\theta_i - \theta_{0,i})^2$$

$$E_{torsion} = \sum_i K[1 + cos(n\emptyset - d)]$$

or

$$E_{torsion} = \sum_i [C_1 + C_2 cos(\emptyset) + C_3(\cos(\emptyset))^2 + C_4(\cos(\emptyset))^3]$$

$$E_{nonbond} = \sum_i \sum_{j>i} \left\{ \frac{q_i q_j e^2}{r_{ij}} + 4\varepsilon_{ij}\left[\left(\frac{\sigma_{ij}}{r_{ij}}\right)^{12} - \left(\frac{\sigma_{ij}}{r_{ij}}\right)^{6}\right]\right\}$$

Here, $k_{b,i}$, $k_{\theta,i}$, represent the bond and angle force constants, respectively. K, C_1, C_2, C_3, and C_4 are torsion energy coefficients, n is the periodicity of the torsion, d is the phase offset, and $\emptyset$ is the dihedral angle. $r_{0,i}$ and $\theta_{0,i}$ are the bond distance and bond angle at equilibrium, respectively. For $E_{nonbond}$, q_i is the partial atomic charge, r_{ij} is the distance between atoms i and j, ε_{ij} and σ_{ij} are the Lennard-Jones parameters which refers to the depth of the potential well and the distance where the potential is zero, respectively. A flexible version of the EPM2[6] force field was used for CO_2, as presented previously[7]. The partial atomic charges for AMP and DEEA were obtained from QM calculations at the B3LYP/6-311+G(d,p) level of theory and using the Merz-Singh-Kollman scheme[8], and were adjusted such that classical MD simulations could reproduce the N-H_{H2O} hydrogen bond interactions observed in AIMD simulations, calculated via radial distribution functions (RDFs). The rest of the force field parameters were obtained from the general Amber force field,[9,10] with the exception of some dihedral parameters obtained from a force field parametrized for ethanolamine[11]. The Coulomb and L-J energies were calculated between atoms separated by three or more bonds. Although most force fields scale the 1-4 L-J and Coulomb energies, in this simulation, they were unscaled as recommended by a previous study to prevent overestimation of intramolecular hydrogen bonding in the alkanolamine

species.[11] The Lorentz-Berthelot combination rule was applied for unlike atom pairs where $\varepsilon_{ij} = \sqrt{\varepsilon_i \varepsilon_i}$ and $\sigma_{ij} = (\sigma_i + \sigma_j)/2$.

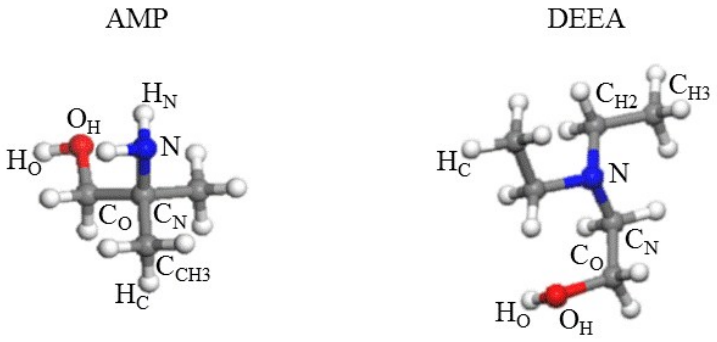

Figure S5. Structures of AMP and DEEA with corresponding atom types for force field parameters listed in Tables S2-S6. Blue, red, grey and white balls represent N, O, C and H atoms, respectively.

Table S3. Nonbonded force field parameters

Species	Atom	q_i	σ_i [Å]	ε_i [kcal mol^{-1}]
AMP	N	-1.003	3.250	0.0157
	C_N	0.625	3.399	0.1700
	C_O	0.112	3.399	0.1094
	C_{CH3}	-0.267	3.399	0.1094
	O_H	-0.653	3.066	0.2104
	H_O	0.395	0.000	0.0000
	H_C	0.0435	2.471	0.0157
	H_N	0.355	1.069	0.0157
DEEA	N	-1.003	3.250	0.1700
	C_N	0.180	3.399	0.1094
	C_O	0.101	3.399	0.1094
	C_{CH2}	0.200	3.399	0.1094
	C_{CH3}	0.080	3.399	0.1094
	O_H	-0.653	3.066	0.2104
	H_O	0.395	0.000	0.0000
	H_C	0.030	2.471	0.0157
CO_2	O	-0.3256	3.033	0.1600
	C	0.6512	2.757	0.0560

Table S4. Bond parameters

Species	Bond Type	k_b [kcal mol^{-1} Å^{-2}]	r_0 [Å]
AMP	$N - H_N$	394.1	1.018
AMP, DEEA	$N - C_N$	320.6	1.470
	$C - C$	303.1	1.535
	$C_O - O_H$	314.1	1.426
	$O_H - H_O$	369.6	0.974
	$C - H_C$	335.9	1.093
CO_2	C-O	1283.38	1.149

Table S5. Angle parameters

Species	Angle Type	k_θ [kcal mol^{-1} rad^{-2}]	θ_0 [°]
AMP	$C_N - N - H_N$	46.0	116.78
	$H_N - N - H_N$	35.0	109.5
AMP, DEEA	$H_C - C - H_C$	35.0	109.5
	$C - C - C$	40.0	109.5
	$H_C - C - O_H$	50.0	109.5
	$N - C - C$	66.2	110.38
	$H_C - C - C$	46.4	110.07
	$C_N - C - O_H$	67.7	109.43
	$C - O_H - H_O$	47.1	108.16
DEEA	$H_C - C - N$	50.0	109.5
CO_2	O-C-O	56.53	180

Table S6. Dihedral parameters (multi-harmonic form)[11]

Species	Dihedral Type	C_1 [kcal mol^{-1}]	C_2 [kcal mol^{-1}]	C_3 [kcal mol^{-1}]	C_4 [kcal mol^{-1}]
AMP	$H_N - N - C_N - C_O$	0.59	-3.75	-1.18	3.28
AMP, DEEA	$O_H - C_O - C_N - N$	0.08	-4.487	-0.16	4.6224
	$C_N - C_O - O_H - H_O$	0.0	-0.22	0.0	-0.28

Table S7. Dihedral parameters (amber form)[9]

Species	Dihedral Type	K [kcal mol^{-1}]	n	d [°]
AMP	$H_C - C_O - O_H - H_O$	0.167	3	0
	$X - C - C - H_C/C$	0.156	3	0
DEEA	C - C - N - C	0.480	2	180

	H_C - C - N - X	0.300	3	0

References

[1] M. Bonomi, D. Branduardi, G. Bussi, C. Camilloni, D. Provasi, P. Raiteri, D. Donadio, F. Marinelli, F. Pietrucci, R. A. Broglia and M. Parrinello, *Comput. Phys. Commun.*, 2009, **180**, 1961–1972.

[2] CPMD, http://www.cpmd.org/, Copyright IBM Corp 1990-2015, Copyright MPI Für Festkörperforschung Stuttgart 1997-2001.

[3] M. E. Tuckerman, A. Chandra and D. Marx, *Acc. Chem. Res.*, 2006, **39**, 151–158.

[4] D. Marx, A. Chandra and M. E. Tuckerman, *Chem. Rev.*, 2010, **110**, 2174–2216.

[5] A. Stirling, *J. Phys. Chem. B*, 2011, **115**, 14683–14687.

[6] J. G. Harris and K. H. Yung, *J. Phys. Chem.*, 1995, **99**, 12021–12024.

[7] S.-N. Huang, T. A. Pascal, W. A. Goddard, P. K. Maiti and S.-T. Lin, *J. Chem. Theory Comput.*, 2011, **7**, 1893–1901.

[8] U. C. Singh and P. A. Kollman, *J. Comput. Chem.*, 1984, **5**, 129–145.

[9] W. D. Cornell, P. Cieplak, C. I. Bayly, I. R. Gould, K. M. Merz, D. M. Ferguson, D. C. Spellmeyer, T. Fox, J. W. Caldwell and P. A. Kollman, *J. Am. Chem. Soc.*, 1995, **117**, 5179–5197.

[10] J. Wang, R. M. Wolf, J. W. Caldwell, P. A. Kollman and D. A. Case, *J. Comput. Chem.*, 2004, **25**, 1157–74.

[11] E. F. da Silva, T. Kuznetsova, B. Kvamme and K. M. Merz, *J. Phys. Chem. B*, 2007, **111**, 3695–3703.